Electronic and optical properties of $Si_{1-y}C_y$ alloys

George Theodorou* and George Tsegas
Department of Physics, Aristotle University of Thessaloniki, 540 06 Thessaloniki, Greece

Pantelis C. Kelires
Physics Department, University of Crete, P.O. Box 2208, 710 03 Heraclion, Crete, Greece
and Foundation for Research and Technology-Hellas (FORTH), P.O. Box 1527, 711 10 Heraclion, Crete, Greece

Efthimios Kaxiras
Department of Physics and Division of Engineering and Applied Sciences, Harvard University, Cambridge, Massachusetts 02138
(Received 14 December 1998; revised manuscript received 14 May 1999)

We investigate the electronic and optical properties of free-standing and epitaxially strained $Si_{1-y}C_y$ alloys. We first determine the microscopic atomic structure of the alloys using the semi-grand-canonical Monte Carlo method and empirical interatomic potentials. For the calculation of the electronic and optical properties of the alloys we employ a supercell geometry and an empirical tight-binding model, which was fitted to reproduce the relevant band structures obtained from first-principles calculations. Our approach allows for a thorough investigation of C alloying and strain effects on the band gap, the band offsets, the effective masses of the upper valence and lowest conduction bands, and the optical properties. Our results are in very good agreement with experiment. [S0163-1829(99)01240-0]

I. INTRODUCTION

Binary group-IV semiconductor alloys have attracted considerable attention in recent years because of their usefulness in electronic devices. The quest for realization of such materials is motivated by the desire to manipulate the band gap of silicon, which can be achieved through alloying or by creating strained-layer superlattices (SL's). A prototypical and extensively studied system is silicon-germanium ($Si_{1-x}Ge_x$) alloys and SL's, usually grown on Si(100) substrates.[1] Another interesting case is the binary silicon-carbon ($Si_{1-y}C_y$) system. In thermodynamic equilibrium the only stable solid solutions that Si and C form are the equimolar perfectly ordered, strain-free zinc-blende (3C-SiC) structure and the various stoichiometric polytypes.[2,3] Nonstoichiometric mixtures of these elements are *metastable*. The solubility of carbon in silicon under equilibrium conditions is extremely small ($\leqslant 2\times 10^{-3}$ at. % at its melting point[4]), because of the huge lattice constant mismatch and the cost in elastic energy (strained bonds) as carbon is incorporated into the lattice. Therefore, experimental efforts to overcome this obstacle have been based on nonequilibrium methods, such as growth of films by molecular beam epitaxy[5,6] and chemical vapor deposition,[7] which exploit the less constrained environment and the higher atomic mobility on surfaces. The goal is to produce pseudomorphic $Si_{1-y}C_y$ layers on or in Si which are free from extended defects, and where the possibility for nucleation of 3C-SiC during growth is kinetically suppressed.[6–8]

The discussion of the electronic properties of $Si_{1-y}C_y$ alloys has been quite controversial. The possibility that incorporation of carbon, which in the diamond bulk phase has a larger band gap than Si, might yield a wide-band-gap Si-based material is appealing. It is, however, not obvious that C incorporation will yield the desired effect. Theoretical arguments based on a linear interpolation scheme of the elemental band gaps indicate that the gap should increase as C is added in Si.[9] Orthogonal linear combination of atomic orbitals calculations based on the virtual-crystal approximation led to the same conclusion.[10] However, tight-binding-like quantum molecular-dynamics calculations, based on localized atomic orbitals and the local-density approximation, indicated that the $Si_{1-y}C_y$ alloys do not follow a mean-field-like (virtual crystal) behavior, as $Si_{1-x}Ge_x$ alloys do, and that the gap actually decreases with C content.[11,12] This reduction was attributed to the incompatibility of the Si and C bonding states which forces the C atoms to act as substitutional point defects, and the C states to behave as localized deep levels in the gap. Similarly, calculations based on the linear-muffin-tin-orbital (LMTO) method found a shrinking of the gap.[13] The latter, LMTO studies, were limited to small cells (16 atoms) and so only high carbon contents could be considered ($>6\%$). This is a serious limitation, because the amount of useful carbon which in practice enters substitutionally into the bulk of the material is limited to below 3%. At higher concentrations, stacking faults and other extended defects appear.

These theoretical studies, although very useful, did not actually focus on *epitaxially strained* alloys, so the effect of biaxial strain which is imposed by the substrate has not been studied and separated from the effect due to the chemical substitution. This makes the interpretation of experimental measurements, where both effects operate, complicated. Experimental work, on the other hand, estimates the influence of epitaxial strain on the gap indirectly by assuming that the deformation potentials of these alloys (actual values are not known) are equal to those of Si, thereby introducing an uncertainty on what is the pure chemical contribution from carbon substitution.

In this paper we investigate by theoretical methods both

strain and chemical effects, and we separate their contributions to the total variation of the band gap as a function of carbon content. Recent photoluminescence studies have provided reliable information about energy shifts in pseudomorphic $Si_{1-y}C_y/Si$ multiple-quantum-well structures.[14,15] In both studies the results were interpreted as indicating that the gap decreases linearly with C content as $\Delta E_g(y) \simeq -y(6.5\ \text{eV})$. The carbon content in these structures was estimated using Vegard's law, which demands that the lattice parameters as well as the elastic constants adhere to a linear interpolation scheme of the elemental constants. Previous theoretical calculations by one of the authors[16–18] showed that for a reliable estimation of the carbon content in both bulk (unstrained) and epitaxially strained $Si_{1-y}C_y$ and $Si_{1-x-y}Ge_xC_y$ alloys, one has to take into account significant deviations of lattice parameters and elastic constants from linearly interpolated values. Failure to do so results in considerable overestimation of C concentration. These predictions for deviations from linear rules were verified both experimentally[19,20] and theoretically.[12] Here we therefore *reinterpret* the experimental intrinsic energy shifts using the corrected carbon content. We find that our theoretical results on the behavior of the band gap are in very good agreement with the reduction of the gap suggested by photoluminescence experiments.

We also considered in detail the optical properties of $Si_{1-y}C_y$ alloys. There is experimental work on this subject,[21] but a theoretical treatment is lacking. We use for both the band gap and optical studies an empirical tight-binding (ETB) method and supercells with periodic boundary conditions. The input configurations to the electronic structure calculations are generated and equilibrated with a Monte Carlo (MC) algorithm within the empirical potential formalism.

The paper is organized as follows: In Sec. II we outline the methodology on which our calculations are based, giving details about the structural models and the ETB method. Section III gives the results and the accompanying discussion, starting with the electronic properties and continuing with the optical properties.

II. METHODOLOGY

In order to study the physics of the systems of interest, it is important that the calculations realistically reproduce certain key aspects. Among these are the way in which C is incorporated in the Si lattice in the proper concentration. Previous work treated $Si_{1-y}C_y$ alloys as random:[11] the occupation of a site by Si or C at a specific concentration was chosen randomly, and then the system was geometrically relaxed. Alternatively, the effects of ordering were taken into account by considering small (eight-atom) cells (Si_7C_1), but this corresponds to high C contents (12.5%) and misrepresents the strain field in the alloy.[11,22] Our investigations are based on 64-atom cells. We concentrate on low carbon contents appropriate for good quality epitaxial films. At such contents the dominant mechanism for carbon incorporation is at substitutional sites. (With increasing C content the amount of interstitial carbon rises and, along with the appearance of stacking defects, seems to be responsible for the degradation in the quality of the material.) The 64-atom supercells allow for the proper C concentrations (1.6% and 3.2%, with one and two C atoms in the cell, respectively), and their equilibrium structural properties can be thoroughly studied with MC simulations. This is described in Sec. II A.

It is also important to be able to study the electronic features of these systems using a dense grid of reciprocal-space points, so that dielectric functions, hole and electron masses and optical properties can be accurately calculated. To this end, we have developed an ETB Hamiltonian, properly parametrized to reproduce the electronic band structure of Si and SiC at various lattice constants relevant to the structure of the Si-C alloys. The use of the ETB method is advantageous over other methods since it makes it possible to study the electronic structure essentially with the same accuracy as the method to which the ETB parameters have been fitted (in our case the density-functional theory with the local-density approximation, including corrections to the energy eigenvalues for the conduction states). This is described in Sec. II B of the present part.

A. Equilibrium structure of Si-C alloys

The alloys considered here are $Si_{0.984}C_{0.016}$, using a $Si_{63}C_1$ supercell, and $Si_{0.968}C_{0.032}$, using a $Si_{62}C_2$ supercell. We considered two types of supercells: (a) cubic, free-floating, which models the unstrained case and allows us to extract information solely about the chemical effect from C incorporation; (b) tetragonally deformed with the lateral dimensions constrained to be those of the Si lattice, which models strained alloys coherently grown on a Si(001) substrate and allows us to extract information about both chemical and strain effects.

The supercells, and the microscopic structure which they simulate, have to comply with two well-established constraints. The first is the correct description of lattice constant and elastic constant deviations from the linear behavior. Specifically, the equilibrium lattice constant $a_0(y)$ of the unstrained alloys, and the perpendicular lattice constant $a_\perp(y)$ of the strained alloys, must be allowed to relax to their optimal values, along with the atomic positions in the cell. Previous theoretical work has instead used Vegard's law for the determination of the lattice constants.[11,13]

The second constraint has to do with the configurational degrees of freedom. It has been independently shown[6,16,17] that there is an oscillatory distribution of carbon-carbon interactions in the bulk of the alloy. Certain C-C distances are totally absent [the first-nearest-neighbor (NN) interaction is energetically very unfavorable] while other configurations (most notably C atoms at third-NN distances) are favored. More recently, first-principles pseudopotential calculations verified this result, and in addition found that the third NN arrangement is also the energetically most favored configuration in the subsurface layers of $Si_{1-y}C_y(100)$ alloys.[23,24] The bulk of the material in such semiconducting systems, where atomic diffusion near the surface is fast while bulk diffusion is negligible, is formed when surface geometries are frozen in during growth. It is therefore essential for the present studies to consider this specific arrangement when there are two carbon atoms in the cell ($Si_{62}C_2$).

In order to comply with the above two constraints we generated our cells, both free floating and epitaxially strained, using a Monte Carlo algorithm[16] specifically devel-

oped to treat the insertion-removal-equilibration processes in alloys with large size mismatch between the constituent atoms. These alloys are *locally* strained in the neighborhood of carbon insertions, even in the free-floating case. This algorithm equilibrates simultaneously both positional and configurational degrees of freedom in the cell, and identifies the most favorable geometries which minimize strain using the *semi-grand-canonical* ensemble. Details of the method are given elsewhere.[25] The energetics of the system are described via the empirical interatomic potentials of Tersoff for multicomponent systems,[26] which have been extensively tested and applied with success in similar contexts.[16–18,23,24] Predictions made in these works have been verified experimentally.[19,20,27] The reliability of the empirical interactions, especially in describing trends in total-energy differences, has been established by comparing to results from first-principles quantum-mechanical calculations.[23,24]

In the strained case, the lateral dimensions are constrained to the lattice constant of bulk Si (the empirical potential used here gives $a_{\mathrm{Si}}=5.432$ Å). In the free-floating case, the relaxed unit cell dimensions yield equilibrium lattice constants a_0 equal to 5.393 and 5.356 Å for the $Si_{0.984}C_{0.016}$ and $Si_{0.968}C_{0.032}$ alloys, respectively. Use of Vegard's law would overestimate a_0, giving 5.403 Å for the first case and 5.373 Å for the second. The theory of elasticity, in conjuction with the free-floating Vegard values for a_0 and linearly interpolated elastic constants,[16,17] for the perpendicular lattice constant $a_\perp$ of the strained alloys, would give values of 5.374 and 5.319 Å, respectively. These are significantly larger than the MC relaxed values 5.352 and 5.271 Å. Thus, use of the linear rules underestimates the tensile strain in the alloys, and as a result overestimates the carbon contents by about 30%. This has important consequences on the discussion of the experimental band-gap shifts.

The interatomic distances in our cells are strongly affected in the neighborhood of carbon insertions. Thus, while the Si-Si distances are close to the corresponding distances for bulk Si, the Si-C distances are considerably different than the corresponding values for the equilibrium 3C-SiC structure. In particular, the first-, second-, and third-neighbor distances of a C atom in 3C-SiC are equal to r_1(C-Si) $=1.87$ Å, r_2(C-C)$=3.05$ Å, and r_3(C-Si)$=3.58$ Å (for $a_{\mathrm{SiC}}=4.32$ Å with the potential used here). For the $Si_{1-y}C_y$ alloys, with $y=0.016$ and $y=0.032$, our calculations give that the distances between a C atom and its first-neighbor Si atoms are distributed around the value of $r_1=1.93$ Å, while the distances to the second-neighbor Si atoms are distributed around the value of $r_2=3.68$ Å. The fact that both distances are larger than the 3C-SiC values reflects the strain induced by carbon incorporation. By extrapolating to the 3C-SiC compound, a distance of $r_1=1.93$ Å for the nearest neighbors corresponds to a lattice constant of 4.45 Å, while a distance of $r_2=3.68$ Å for the next-nearest neighbors to a lattice constant of 5.2 Å. Both of these values are considerably larger than the equilibrium lattice constant for crystalline bulk 3C-SiC (4.32 Å).

B. Methods for electronic properties

The Si-C distances in the $Si_{1-y}C_y$ alloys under consideration are considerably different than the corresponding distances for the equilibrium 3C-SiC compound. Consequently, to obtain the appropriate tight-binding parameters for the alloys of interest we performed first-principles calculations for the band structure of 3C-SiC compounds with lattice constants 4.45 and 5.2 Å. The calculations were based on the density-functional theory (DFT) in the local-density approximation (LDA).[28] The atomic cores are represented by nonlocal norm-conserving pseudopotentials of Bachelet *et al.*[29] We use plane waves with a cutoff of 48 Ry to expand the wave functions and the potentials and a grid of $6\times6\times6$ **k** points of the Monkhorst-Pack type[30] in the full Brillouin Zone (BZ). As is well known, the energies of conduction states are not well reproduced by the DFT/LDA approach.[31] For this reason, we have used the recently introduced generalized density-functional theory (GDFT) correction to DFT/LDA eigenvalues.[32] A recent thorough study of the applicability of GDFT[33] concluded that it gives reasonable results for the band gap of many semiconductor compounds containing elements from the second to fourth rows of the Periodic Table (accurate to about 10% of the experimental values or better). In particular, the GDFT corrections to DFT/LDA eigenvalues work rather satisfactorily for the system considered in the present work.[33,34] The band structure from the GDFT/LDA calculations is shown in Fig. 1. Spin-orbit coupling has not been taken into account in these calculations. For a lattice constant $a=4.45$ Å the material is an

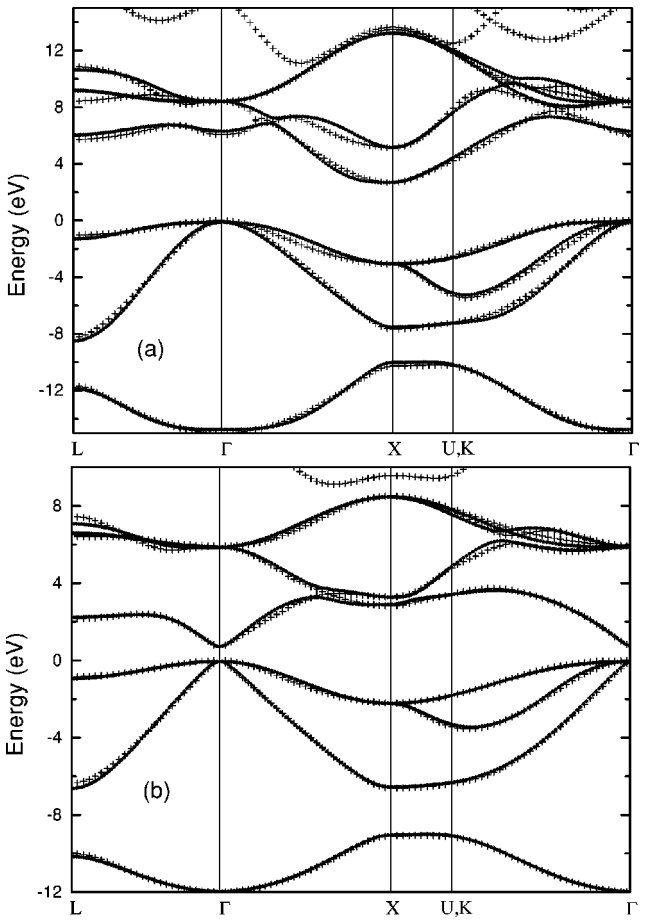

FIG. 1. Band structure for the 3C-SiC compound with lattice constants (a) 4.45 and (b) 5.2 Å, calculated using the GDFT/LDA method (+) and the ETB method (●), without taking spin-orbit coupling into account.

TABLE I. ETB model interaction parameters (in eV) for 3C-SiC at lattice constants 4.45 and 5.2 Å. The notation is that of Slater and Koster.

	$a=4.45$ Å	$a=5.2$ Å		$a=4.45$ Å	$a=5.2$ Å
E_{ss}^{c}	0.8179	0.2142	$E_{ss}^{c}(0.5,0.5,0.0)$	0.38370	−0.00812
E_{pp}^{c}	4.0145	3.3105	$E_{sx}^{c}(0.0,0.5,0.5)$	−0.65192	−0.18688
E_{ss}^{a}	−9.9689	−7.5077	$E_{sx}^{c}(0.5,0.5,0.0)$	−0.15261	0.07828
E_{pp}^{a}	3.0260	0.3765	$E_{xx}^{c}(0.5,0.5,0.0)$	0.39595	0.32195
			$E_{xx}^{c}(0.0,0.5,0.5)$	0.11434	−0.07541
$E_{ss}(0.25,0.25,0.25)$	−1.04358	−0.66784	$E_{xy}^{c}(0.5,0.5,0.0)$	0.12471	0.33869
$E_{sx}(0.25,0.25,0.25)$	0.98851	1.29551	$E_{xy}^{c}(0.0,0.5,0.5)$	0.15909	−0.10041
$E_{xs}(0.25,0.25,0.25)$	−1.57999	−1.06044	$E_{ss}^{a}(0.5,0.5,0.0)$	−0.32872	−0.32229
$E_{xx}(0.25,0.25,0.25)$	0.60537	0.30846	$E_{sx}^{a}(0.0,0.5,0.5)$	−0.48714	−0.52365
$E_{xy}(0.25,0.25,0.25)$	1.99905	1.33008	$E_{sx}^{a}(0.5,0.5,0.0)$	−0.59686	−0.36154
			$E_{xx}^{a}(0.5,0.5,0.0)$	0.14400	0.25805
			$E_{xx}^{a}(0.0,0.5,0.5)$	−0.88910	−0.55811
			$E_{xy}^{a}(0.5,0.5,0.0)$	0.08043	0.14910
			$E_{xy}^{a}(0.0,0.5,0.5)$	−0.46023	−0.35665

indirect gap semiconductor with a fundamental gap at X of $E_g^i=2.685$ eV, and a direct gap at Γ of $E_g^d(\Gamma)=6.054$ eV; for $a=5.2$ Å it becomes a direct gap semiconductor with a gap equal to $E_g=0.767$ eV.

Our intention is to use the ETB method as developed by one of the authors and his collaborators,[35–37] in order to reproduce the GDFT/LDA results. This method is based on a model Hamiltonian, in the three-center representation, with an orthogonal sp^3 set of orbitals and interactions up to third neighbor for Si and second neighbor for 3C-SiC. The interaction parameters of Ref. 35 are used for bulk Si, while the values of the interaction parameters for 3C-SiC compounds with lattice constants of 4.45 and 5.2 Å are determined by fitting the band-structure results of the GDFT/LDA calculations discussed above. The interaction parameters obtained in that way are listed in Table I. The resulting band structure from the ETB calculations for the above 3C-SiC compounds is shown in Fig. 1. From this figure we conclude that the ETB model describes very well not only the valence bands but also the lowest conduction bands.

For the calculation of the electronic and optical properties of $Si_{1-y}C_y$ alloys, the ETB Hamiltonian matrix elements are needed. The on-site matrix elements (atomic term values) for Si orbitals are taken from the corresponding ones for bulk Si, while those for C orbitals from the 3C-SiC compound with a lattice constant of 4.45 Å. The resulting mean difference between the Si and C atomic term values (ATV difference) is 0.33 eV. The corresponding difference for the equilibrium 3C-SiC compound is[34] 3.4 eV, and that for isolated Si and C atoms[38] is 2.3 eV. From these comparisons we conclude that for $Si_{1-y}C_y$ alloys a reasonable value for the ATV difference is 3 eV, and the C atomic term values are accordingly shifted by the appropriate amount. In addition, for the $Si_{1-y}C_y$ alloys, there is some randomness in the interatomic distances, implying a modification of the Hamiltonian matrix elements between orbitals located on different atoms. This modification is taken into account with the scaling formula[35,37]

$$H_{\alpha,\beta}(d)=H_{\alpha,\beta}(d_0)(d_0/d)^{\nu_{\alpha\beta}}. \quad (1)$$

The values for the scaling indices ν_{ss}, ν_{sp}, and ν_{pp} are taken equal to 3, 1.8, and 1, respectively, for both Si and C. Moreover, Hamiltonian matrix elements between C and Si orbitals localized on atoms at a second-nearest-neighbor distance cannot be obtained from the 3C-SiC interaction parameters, since in the latter case no second-nearest-neighbor C-Si interactions exist. The corresponding C-Si Hamiltonian matrix elements are estimated as the mean value of C-C and Si-Si matrix elements at the appropriate distance. Finally, for biaxial strain parallel to the (001) plane, a modification of the on-site p-orbital integrals $E_p^{x,y}$ and E_p^z for the p_x, p_y, and p_z orbitals is taken into account by the linear formulas

$$E_p^{x,y}=E_p+b_p(\epsilon_\parallel-\epsilon_\perp), \quad E_p^z=E_p-2b_p(\epsilon_\parallel-\epsilon_\perp), \quad (2)$$

where $\epsilon_\parallel$ and $\epsilon_\perp$ are the strain components parallel and perpendicular to the biaxial plane. The parameter b_p is taken to be 2 eV for Si and 1 eV for C atoms.

III. RESULTS AND DISCUSSION

A. Electronic properties

Band structure. Our goal in studying the band structure of $Si_{1-y}C_y$ alloys is twofold: to examine if the general trend for reduction of the fundamental band gap with increasing carbon content holds (as suggested both from experiment[14,15] and by previous theoretical work[11,13,22]), and to separate in this variation the chemical and strain contributions. To extract the pure chemical contribution from carbon incorporation, we compared the band structure of crystalline Si, calculated using also a 64-atom cubic supercell Si_{64}, with the band structures of the free-floating $Si_{1-y}C_y$ cells described in Sec. II. The band structure of crystalline Si_{64}, along the symmetry lines of the BZ of the supercell is shown in Fig. 2(a) (the BZ for the simple cubic lattice is given as inset). The band structure of Si_{64} is related to that of Si in the standard fcc unit cell by zone folding. In Fig. 2(b) we give the band structure of the unstrained (free-floating) $Si_{0.968}C_{0.032}$. The minimum of the conduction band in both cases is along the ΓX direction, and the gap is equal to 1.052 eV for the Si_{64}

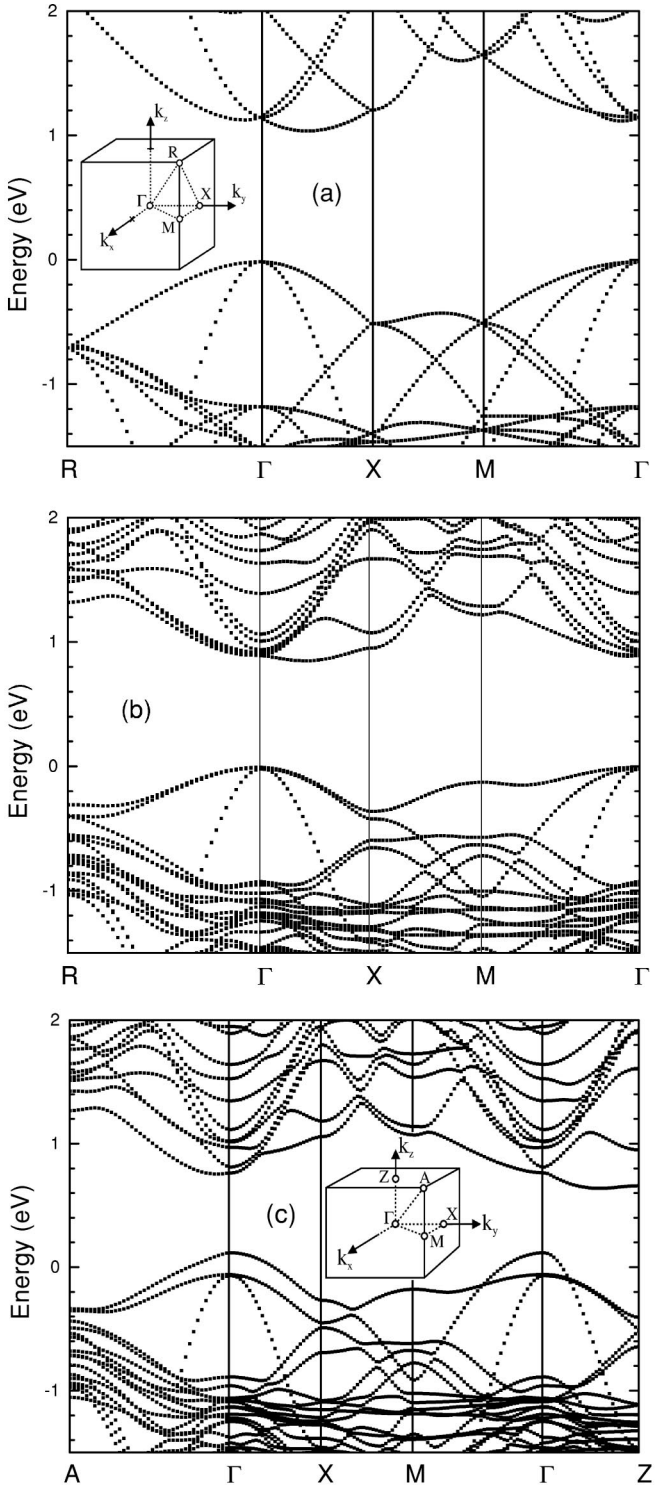

FIG. 2. Band structure for (a) bulk Si_{64}, (b) unstrained $Si_{0.968}C_{0.032}$, and (c) strained $Si_{0.968}C_{0.032}$, calculated using the ETB method, without taking spin-orbit coupling into account. The insets are the corresponding Brillouin zones.

cell and 0.826 eV for the $Si_{0.968}C_{0.032}$ alloy. The fundamental gap for the unstrained $Si_{0.968}C_{0.032}$ alloy is smaller than the corresponding one for Si_{64} by 0.226 eV. This confirms that the effect of adding carbon in the Si lattice is to shrink the gap. The reduction is quantified by defining the coefficient $\gamma = -\Delta E_g(y)/y$, where y is the concentration of C in the alloy. For a reduction of the gap of 0.226 eV and $y = 0.032$ we have $\gamma = 7$ eV. This represents the chemical contribution to the variation of the band gap of the alloy with C content. A similar value is obtained from the investigation of the free-floating $Si_{0.984}C_{0.016}$ alloy, $\gamma = 7.6$ eV.

Previous theoretical work also predicted reduction of the gap with increasing C concentration. The work of Ref. 13 was performed using 16-atom cells, which are too small with correspondingly high C content. Extrapolation to lower C content is not possible from these studies. Some comparison can be made with the work of Ref. 11, which was done for unstrained alloys, using 64-atom cells. According to these calculations, the $Si_{0.984}C_{0.016}$ alloy exhibits conduction band minima at the Γ and R points of the BZ, and a reduction of the fundamental gap relative to Si_{64} equal to 0.45 eV, giving $\gamma = 28$ eV, a value four times larger than that predicted by our calculations.

By investigating the epitaxially strained alloys, where both strain and chemical contributions are present, we are in a position to deduce direct information about the epitaxial strain effects through comparison to the free-floating case. Let us focus on the strained $Si_{0.968}C_{0.032}$ (s-$Si_{0.968}C_{0.032}$) alloy. The band structure of s-$Si_{0.968}C_{0.032}$ is shown in Fig. 2(c) [the BZ of the strained material is tetragonal, shown as an inset in Fig. 2(c)]. Strain reduces the fundamental gap of the material, which is located along the ΓZ direction. The modification of the band gap, relative to crystalline Si_{64}, is now $\Delta E_g = -0.53$ eV, giving the value $\gamma = 17$ eV. This value includes both the chemical and the strain contributions. Assuming that the two contributions are additive, we conclude that the strain contribution is 10 eV, that is, somewhat stronger than the chemical contribution. For comparison, the work of Ref. 12 predicts that the s-$Si_{0.984}C_{0.016}$ alloy exhibits a deep-level conduction band, with a minimum at the Γ and R points of the BZ and a band gap smaller by 0.67 eV in comparison to that of Si_{64}, giving a very large value for γ ($\gamma = 43$ eV). As stated by the authors of Ref. 12, the existence of such a deep-level band is difficult to be proven experimentally, since many other defects display lines in the region. In addition, our calculations do not predict such a band. In the calculations of Ref. 12, the next conduction band above the deep-level band is very similar to the lowest conduction band of pure Si, with the corresponding band gap found 0.26 eV smaller than their result for Si_{64}, giving a value of $\gamma = 16.25$ eV, in excellent agreement with our results.

In the previous calculations, the mean value for the ATV difference between Si and C atoms was taken to be 3 eV. Since the exact value for this quantity is not known, calculations for γ were carried out for a range of values for the ATV difference, from 0 to 4 eV. The results of these calculations are shown in Fig. 3. The coefficient γ increases with the increase of the ATV difference, going from 13.5 to 19.8 eV for values of the ATV difference from 0 to 4 eV.

Effective masses. The effective masses for the upper valence and lower conduction bands were calculated using the present ETB model. In order to estimate the accuracy of the model, the effective masses for the heavy-hole (hh), light-hole (lh), and spin-hole (sh) states, and the electron state at the minimum of the conduction band for bulk Si, were calculated and compared with experiment. The results are

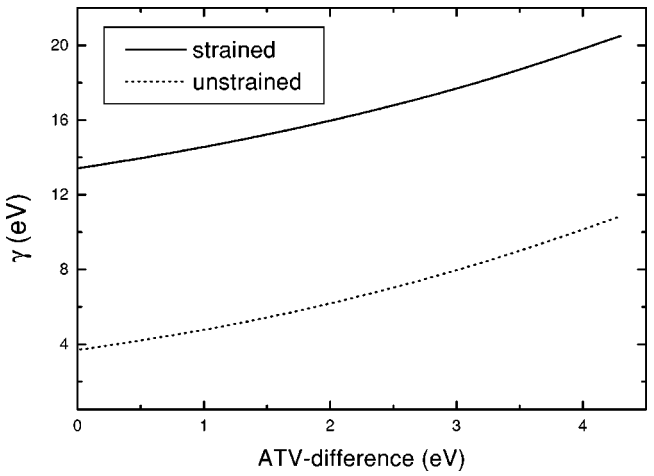

FIG. 3. Calculated ratio $\gamma = -\Delta E_g(y)/y$ for a range of values of the ATV difference between Si and C, from 0 to 4 eV.

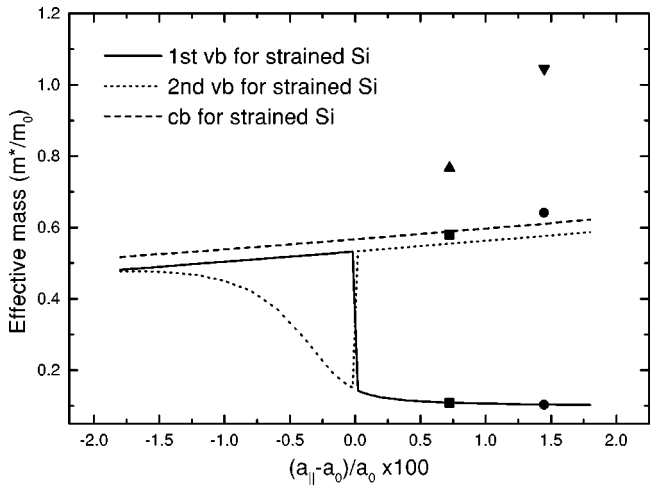

FIG. 4. The effective masses for the two upper valence bands (vb's) and the lowest conduction band (cb) for biaxially strained Si, as a function of the strain in the biaxial plane, $\epsilon_\parallel = (a_\parallel - a_0)/a_0$. We also include the effective masses for the two upper valence bands and lowest conduction bands for (a) s-$Si_{0.984}C_{0.016}$ (■ for the vb's and ▲ for the cb) and (b) the s-$Si_{0.968}C_{0.032}$ (● for the vb's and ▼ for the cb).

shown in Table II. With the exception of the longitudinal effective mass at the conduction band minimum, m_L^*, the agreement between theory and experiment is excellent. For the case of m_L^*, the present model underestimates the value of the effective mass by about 40%. In Table II we list the calculated effective masses for the alloys $Si_{0.984}C_{0.016}$ and $Si_{0.968}C_{0.032}$, both unstrained and strained [coherently grown on a Si (001) substrate]. For the unstrained case the lh, hh, and sh effective masses have very similar values. For the strained alloys, the sh effective mass in the [100] direction is close to that of the lh, while in the [001] direction it is close to the hh effective mass.

The effective masses in the [001] direction for strained alloys are also shown in Fig. 4, together with the effective mass of Si under biaxial strain. The valence-band effective masses are plotted as a function of the strain in the biaxial plane $\epsilon_\parallel = (a_\parallel - a_0)/a_0$, with a_0 the lattice constant of the unstrained material and $a_\parallel$ the lattice constant of the strained material in the biaxial plane. For positive strain, $\epsilon_\parallel > 0$, (negative strain, $\epsilon_\parallel < 0$) the highest valence band for Si is the lh band (hh band). The results of the calculations show that for the alloys the lh effective mass is very close to that for strained Si under the same biaxial strain, the hh effective mass shows a small deviation from the corresponding one for strained Si, while the electron longitudinal effective mass is strongly influenced by the C atoms.

Band offsets. An important parameter for applications is the valence-band offset (VBO) as well as the conduction-band offset (CBO) for the $Si(001)/Si_{1-y}C_y$ interfaces. Before proceeding with the study of the $Si(001)/Si_{1-y}C_y$ interface, and for the verification of the accuracy of the method, in Fig. 5 we present the results of the calculations, using the ETB method, for the variation of the top of the valence band as well as the minimum of the conduction band, for Si under biaxial strain. The results are given as a function of the strain in the biaxial plane. In the same figure we also show the results of the deformation potential theory, produced using the values[40] $b = -2.1$ eV and $\Xi_d^\Delta + \frac{1}{2}\Xi_u^\Delta - a_v = 1.5$ eV for the deformation potentials, and the value[41] of 1.8 eV for the absolute deformation potential a_v. The agreement between the ETB model and deformation potential theory is very good for the hh, lh, and sh states. For the minimum of the conduction band along the [001] direction, Δ_z, the ETB model overestimates the value of the reduction for the conduction band minimum by a factor of about 1.5. From these results we conclude that the ETB model will provide good results for the VBO of the $Si(001)/Si_{1-y}C_y$ interface, but will overestimate the values of the CBO.

The calculated band alignment for the $Si(001)/Si_{1-y}C_y$ interface is of type I, with holes and electrons localized in the

TABLE II. $Si_{1-y}C_y$ effective masses, in units of m_0, for the lh, hh, and sh bands along the [100] and [001] directions, and longitudinal m_L^* and transverse m_T^* electron effective masses at the minimum of the conduction band in the direction [001] (Δ_z).

y (%)	$m_{lh}^*[100]$	$m_{hh}^*[100]$	$m_{sh}^*[100]$	$m_{lh}^*[001]$	$m_{hh}^*[001]$	$m_{sh}^*[001]$	$m_L^*(\Delta_z)$	$m_T^*(\Delta_z)$
0.0 (unstrained)	0.147	0.533	0.234	0.147	0.533	0.234	0.567	0.173
[Expt. (Ref. 39)]	0.153	0.537	0.234	0.153	0.537	0.234	0.916	0.191
1.6 (unstrained)	0.220	0.244	0.236	0.220	0.244	0.236	0.744	0.173
(strained)	0.176	0.517	0.182	0.108	0.580	0.518	0.767	0.167
3.2 (unstrained)	0.210	0.270	0.240	0.210	0.270	0.240	0.802	0.180
(strained)	0.175	0.56	0.18	0.103	0.640	0.623	1.045	0.165

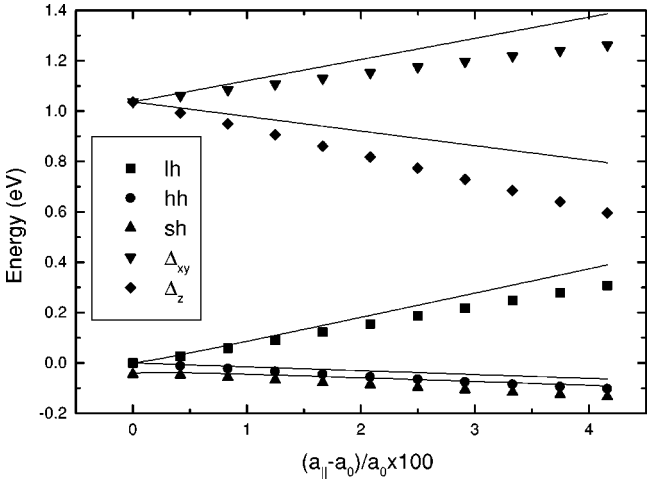

FIG. 5. Energies of the three top valence states at the Γ point, and the lowest conduction states at Δ_z and Δ_{xy}, for biaxially strained Si. The points in the figure represent values obtained from the ETB model, while the lines represent values from deformation potential theory.

$Si_{1-y}C_y$ layer. Figure 6 gives the results for the values of the VBO and CBO for the $Si(001)/Si_{0.984}C_{0.016}$ interface, produced by the ETB method. The results are given as a function of the ATV difference between Si and C. From these results we conclude that the VBO is independent of the ATV difference, while the CBO increases with increasing ATV difference. For a reasonable value of the ATV difference, equal to 3 eV, we obtain a VBO of 60 meV and a CBO of 200 meV. On the basis of preceding results for strained Si, the calculated value of the CBO is expected to be overestimated by a factor of about 1.5; taking this into account, we obtain a more realistic value for the CBO of about 130 meV. In conclusion, the calculations imply type-I band alignment with a CBO about 70% of the total band offset.

Comparison with experiment. From the preceding calculations, we found that the band gap of the strained $Si_{1-y}C_y$ alloys coherently grown on a Si(001) substrate varies with

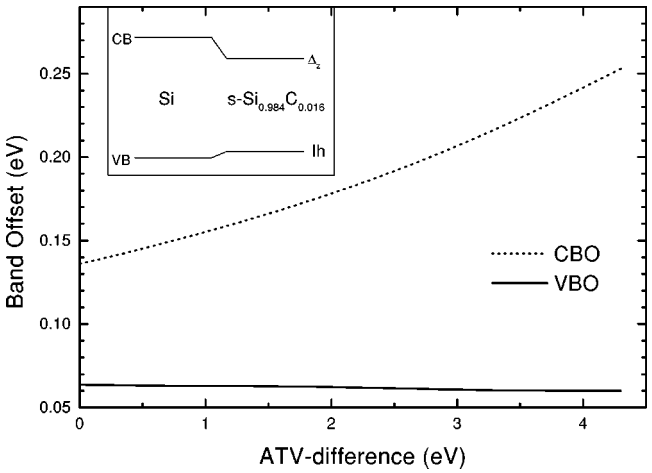

FIG. 6. Absolute values for the valence- and conduction-band offsets for the $Si(001)/Si_{0.984}C_{0.016}$ interface as a function of the ATV difference between Si and C, calculated by the ETB model. The inset shows the band alignment for the $Si(001)/Si_{0.984}C_{0.016}$ interface.

the C concentration according to the relation $\gamma = -\Delta E_g(y)/y = 17$ eV, and that the relative ratio of chemical to strain contribution is $7/10 = 0.7$. In addition, we found that the ETB method overestimates the reduction of the conduction-band minimum due to strain by a factor of about 1.5. For the case of the strained $Si_{0.984}C_{0.016}$ alloy, the corrected CBO is equal to 130 meV, and the corrected reduction of the band gap 209 meV, which leads to a corrected value $\gamma = 13$ eV. The free-floating cells, however, from which the chemical contribution to γ of 7 eV is extracted, are also *locally strained* around the C atoms, with a certain fraction of the bonds deviating from their equilibrium (unstretched) values. Therefore, a similar correction (to the reduction of the conduction band minimum), as made above, should also be applied in the free-floating case. This would lead to some reduction of the chemical contribution too. It is not straightforward in the ETB model to estimate this reduction because the two effects, atom replacement and intrinsic local strain, are intertwined. We can make an estimate of the strain contribution to γ by using deformation potential theory, which for the $Si_{0.984}C_{0.016}$ alloy gives the contribution of 8 eV. Then the chemical contribution is 5 eV, and the ratio of the chemical to strain contribution is now $5/8 = 0.62$, reasonably close to the previously estimated value of 0.7. This is consistent with the experimental photoluminescence studies[14,15] which find a strain contribution larger than the chemical one.

To make a more quantitative comparison with the experimental findings, we must take into account that the experiment is done with a $Si(001)/Si_{1-y}C_y$ quantum well device,[14,15] e.g., a multiple-quantum-well structure with a $Si_{1-y}C_y$ width of 52 Å. Accordingly, we must extrapolate our results to make them compatible with such a multiple-well structure. For the case of a $Si(001)/Si_{0.984}C_{0.016}$ quantum well, we found that the electrons and holes are confined in the alloy layer, with the electron well having a depth of 130 meV and the hole well a depth of 60 meV. Because of quantum effects, the electron energy lies above the bottom of the well, and the hole energies below its bottom. For a quantum well width of 52 Å and an electron effective mass of $0.92m_0$, the increase of the energy level of the electrons in the well, due to quantum confinement, is equal to 15 meV, while for the light hole with an effective mass of $0.1m_0$ the decrease of the energy level is 40 meV. Then the reduction of the gap in the quantum-well structure will be 154 meV, giving a value $\gamma = 9.6$ eV. The reported measured value for the multiple quantum well structure with an alloy-well width of 52 Å is $\gamma = 6.5$ eV. As mentioned in Sec. I, however, this value is deduced from the photoluminescence energy shifts using carbon contents which are *overestimated* by about 30%. If we correct for this overestimation, the experimental value becomes $\gamma = 9.3$ eV, very close to our result. Although there are some uncertainties in both our theoretical approach and the interpretation of the experimental results, we consider this as an excellent agreement between theory and experiment. Finally, we have predicted that about 70% of the band offset is located in the conduction band and 30% in the valence. This is in excellent agreement with the experimental results of Williams *et al.*[42] On the other hand, the experimental results of Kim *et al.*[43] indicate that there is almost no measurable VBO.

B. Optical properties

Finally, we discuss the optical properties of the alloys. For the calculation of the imaginary part, $\varepsilon_2(\omega)$, of the dielectric function we use the expression[44]

$$\varepsilon_2(\omega)=\frac{4\pi^2e^2}{m^2\omega^2}\sum_{c,v}\int\frac{2}{(2\pi)^3}|\langle\mathbf{k},c|\mathbf{P}\cdot\mathbf{a}|\mathbf{k},v\rangle|^2 \times\delta[E_{cv}(\mathbf{k})-\hbar\omega]d\mathbf{k}, \quad (3)$$

where $|\mathbf{k},c\rangle$ and $|\mathbf{k},v\rangle$ are the wave functions of the conduction and valence bands, respectively, $E_{cv}(\mathbf{k})$ is the energy difference between the c (conduction) and v (valence) bands, $\mathbf{P}$ is the momentum operator, and $\mathbf{a}$ the polarization unit vector. In our ETB scheme the momentum matrix elements are expressed in terms of the Hamiltonian matrix elements and distances between localized orbitals.[45,46,36] The integration in the BZ of the supercell is performed within the linear analytic tetrahedron method[47,48] by using a uniform mesh of $8\times8\times8$ $\mathbf{k}$ points. The real part of the dielectric function, $\varepsilon(\omega)$, is obtained by a Kramers-Kronig analysis.

The dielectric function of bulk Si with the present ETB was investigated in detail by Tserbak *et al.*,[35] where it was found that the results of the calculation are in good agreement with experiment. In the present work we have calculated the dielectric function of Si using a cubic supercell of 64 atoms (Si_{64}). The results of the calculations are given in Fig. 7(a). In the same figure we also give the dielectric function for the unstrained $Si_{0.984}C_{0.016}$ and $Si_{0.968}C_{0.032}$ alloys, calculated with the use of a 64-atom cubic supercell. The consequences of the disorder in the alloy, are apparent in the dielectric function: disorder leads to broader peaks and introduces a tail in ε_2 below the direct gap of Si at 3.4 eV. In addition, we found that disorder shifts the E_2 peak, located at 4.3 eV, to lower energies while the position of the E_1 gap, located at 3.5 eV, remains more or less unaffected.

For the strained $Si_{1-y}C_y$ alloy grown coherently on a Si(001) substrate, with a tetragonal crystal structure, the dielectric function exhibits a small anisotropy between polarizations parallel and perpendicular to the growth direction. The dielectric function averaged over the two polarizations is shown in Fig. 7(b) for the strained $Si_{0.984}C_{0.016}$ and $Si_{0.968}C_{0.032}$ alloys, together with the dielectric function of crystalline Si_{64}, while the inset shows the anisotropy between the parallel and perpendicular polarization for the first alloy. The polarization anisotropy is relatively small, with the strongest part between at the critical points E_0' and E_2. The characteristics of the dielectric function curves are similar to those for the unstrained alloy. In particular the position of the E_2 peak shifts with carbon content to lower energies in agreement with experimental data,[21] while we predict that the position of the E_1 gap remains relatively unaffected. In the latter case the experimental data show a small shift to higher energies with carbon content.[21,49]

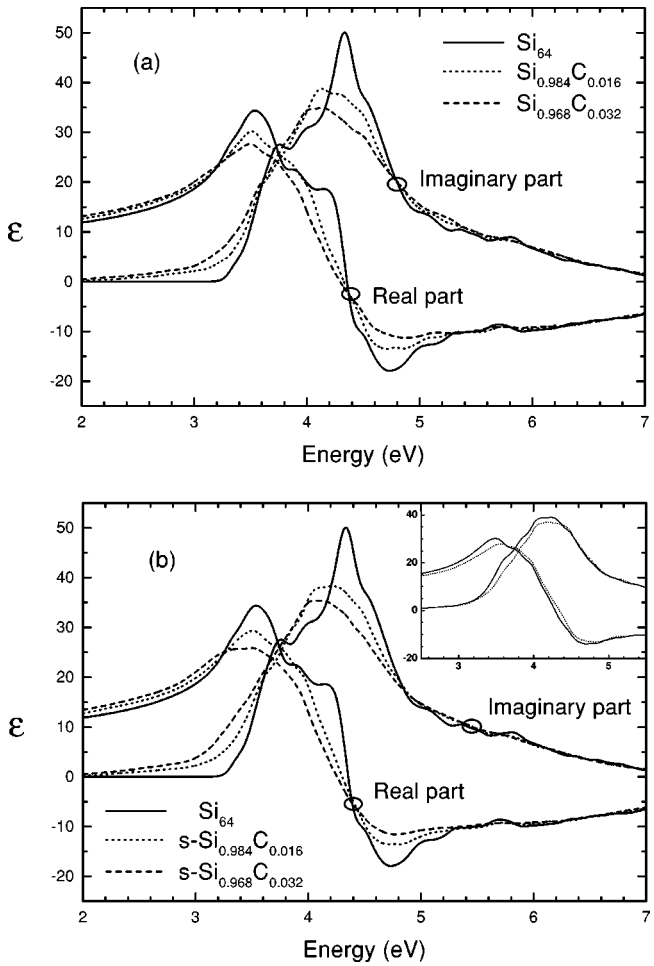

FIG. 7. (a) Calculated real and imaginary parts of the dielectric function for bulk Si_{64}, unstrained $Si_{0.968}C_{0.032}$, and unstrained $Si_{0.968}C_{0.032}$ alloy. (b) Same as in (a) for the strained alloys. For the strained alloys the average dielectric function for the three different polarizations is given. The inset in (b) shows the polarization anisotropy in the dielectric function for a strained $Si_{0.984}C_{0.016}$ alloy, for polarization parallel (solid line) and perpendicular (dotted line) to the biaxial plane.

ACKNOWLEDGMENTS

This work has been supported in part by the Greek Government Secretariat for Research and Technology. E.K. is grateful to the Foundation for Research and Technology Hellas (FORTH), where part of this work was performed, for its hospitality and to the Physics Department of the University of Crete, Heraklion, for the use of resources of the Computational Center.

*Electronic address: theodoru@ccf.auth.gr

[1] *Properties of Strained and Relaxed Silicon/Germanium*, edited by E. Kasper, EMIS Data Review Series No. 12 (INSPEC, London, 1995).

[2] P. J. H. Denteneer and W. van Haeringen, Phys. Rev. B **33**, 2831 (1986).

[3] K. J. Chang and M. L. Cohen, Phys. Rev. B **35**, 8196 (1987).

[4] R. W. Olesinski and G. J. Abbaschian, Bull. Alloy Phase Diagrams **5**, 485 (1984).

[5] S. S. Iyer, K. Eberl, M. S. Goorsky, F. K. LeGoues, J. C. Tsang, and F. Cardone, Appl. Phys. Lett. **60**, 356 (1992).

[6] H. Rücker, M. Methfessel, E. Bugiel, and H. J. Osten, Phys. Rev. Lett. **72**, 3578 (1994).

[7] J. B. Posthill, R. A. Rudder, S. V. Hattangady, G. G. Fountain,

and R. J. Markunas, Appl. Phys. Lett. **56**, 734 (1990).
[8] H. J. Osten, M. Methfessel, G. Lippert, and H. Rücker, Phys. Rev. B **52**, 12 179 (1995).
[9] R. A. Soref, J. Appl. Phys. **70**, 2470 (1991).
[10] B. A. Orner and J. Kolodzey, J. Appl. Phys. **81**, 6773 (1997).
[11] A. A. Demkov and O. F. Sankey, Phys. Rev. B **48**, 2207 (1993).
[12] W. Windl, O. F. Sankey, and J. Menendez, Phys. Rev. B **57**, 2431 (1998).
[13] J. Xie, K. Zhang, and X. Xie, J. Appl. Phys. **77**, 3868 (1995).
[14] K. Brunner, K. Eberl, and W. Winter, Phys. Rev. Lett. **76**, 303 (1996); K. Eberl, K. Bruner, and W. Winter, Thin Solid Films **294**, 98 (1997).
[15] O. G. Schmidt and K. Eberl, Phys. Rev. Lett. **80**, 3396 (1998).
[16] P. C. Kelires, Phys. Rev. Lett. **75**, 1114 (1995).
[17] P. C. Kelires, Appl. Surf. Sci. **102**, 12 (1996).
[18] P. C. Kelires, Phys. Rev. B **55**, 8784 (1997).
[19] M. Meléndez-Lira, J. Menéndez, W. Windl, O. F. Sankey, G. S. Spencer, S. Sego, R. B. Culbertson, A. E. Bair, and T. L. Alford, Phys. Rev. B **54**, 12 866 (1996).
[20] M. Berti, D. De Salvador, A. V. Drigo, F. Romanato, J. Stangl, S. Zerlauth, F. Schaffler, and G. Bauer, Appl. Phys. Lett. **72**, 13 (1998).
[21] W. Kissinger, M. Weidner, H. J. Osten, and M. Eichler, Appl. Phys. Lett. **65**, 3356 (1994).
[22] J. Gryko and O. F. Sankey, Phys. Rev. B **51**, 7295 (1995).
[23] P. C. Kelires and E. Kaxiras, Phys. Rev. Lett. **78**, 3479 (1997).
[24] P. C. Kelires and E. Kaxiras, J. Vac. Sci. Technol. **16**, 1687 (1998).
[25] P. C. Kelires, Int. J. Mod. Phys. C **9**, 357 (1998).
[26] J. Tersoff, Phys. Rev. B **39**, 5566 (1989).
[27] H. Jacobson, J. Xiang, N. Herbots, S. Whaley, P. Ye, and S. Hearne, J. Appl. Phys. **81**, 3081 (1997).
[28] P. Hohenberg and W. Kohn, Phys. Rev. **136**, B864 (1964); W. Kohn and L. J. Sham, Phys. Rev. **140**, A1133 (1965).
[29] G. B. Bachelet, D. R. Hamann, and M. Schlüter, Phys. Rev. B **26**, 4199 (1982).
[30] H. J. Monkhorst and J. D. Pack, Phys. Rev. B **13**, 5188 (1976).
[31] See the original work of M. Hybertsen and S. Louie, Phys. Rev. Lett. **55**, 1418 (1985); Phys. Rev. B **34**, 5390 (1986); R. Godby, M. Schlüter, and L. Sham, Phys. Rev. Lett. **56**, 2415 (1986); Phys. Rev. B **37**, 10 159 (1988).
[32] L. Fritsche, Physica B **172**, 7 (1991); L. Fritsche, C. Kroner, and T. Reinert, J. Phys. B **25**, 4287 (1992); L. Fritsche, Int. J. Quantum Chem. **48**, 185 (1993); L. Fritsche and Y. M. Gu, Phys. Rev. B **48**, 4250 (1993).
[33] I. N. Remediakis and E. Kaxiras, Phys.Rev. B **59**, 5536 (1999).
[34] G. Theodorou, G. Tsegas, and E. Kaxiras, J. Appl. Phys. **85**, 2179 (1999).
[35] C. Tserbak, H. M. Polatoglou, and G. Theodorou, Phys. Rev. B **47**, 7104 (1993).
[36] C. Tserbak and G. Theodorou, Phys. Rev. B **50**, 18 179 (1994).
[37] C. Tserbak and G. Theodorou, Phys. Rev. B **52**, 12 232 (1995).
[38] F. Herman and S. Skillman, *Atomic Structure Calculations* (Prentice Hall, Englewood Cliffs, NJ, 1963).
[39] *Semiconductors. Physics of Group IV Elements and III-V Compounds*, edited by O. Madelung, M. Schulz, and M. Weiss, Landolt-Börnstein, New Series, Group III, Vol. 17, Pt. a (Springer, Berlin, 1982).
[40] L. D. Laude, F. H. Pollak, and M. Cardona, Phys. Rev. B **15**, 2127 (1977).
[41] G. S. Cargill, J. Angilello, and K. L. Kavaragh, Phys. Rev. Lett. **61**, 1748 (1988).
[42] R. L. Williams, G. C. Aers, N. L. Rowell, K. Brunner, W. Winter, and K. Eberl, Appl. Phys. Lett. **72**, 1320 (1998).
[43] M. Kim and H. J. Osten, Appl. Phys. Lett. **70**, 2702 (1997).
[44] F. Wooten, *Optical Properties of Solids* (Academic Press, New York 1972).
[45] N. V. Smith, Phys. Rev. B **19**, 5019 (1979).
[46] L. Brey and C. Tejedor, Solid State Commun. **48**, 403 (1983).
[47] O. Jepsen and O. K. Andersen, Solid State Commun. **9**, 1763 (1971).
[48] G. Lehmann and M. Tauc, Phys. Status Solidi B **54**, 469 (1972).
[49] S. Zollner, C. M. Herzinger, J. A. Woollam, S. S. Iyer, A. P. Powell, and K. Eberl, Solid State Commun. **96**, 305 (1995).